First Search for High-Energy Neutrino Emission from Galaxy Mergers

Subhadip Bouri, Priyank Parashari, Mousumi Das, Ranjan Laha

arXiv 2404.06539

Department of Physics and Centre for High Energy Physics

IISc Bangalore

PPC 2024

14 -18 October 2024, Hyderabad, India

INDIAN INSTITUTE OF SCIENCE

भारतीय विज्ञान संस्थान

What are the sources of Cosmic Rays?

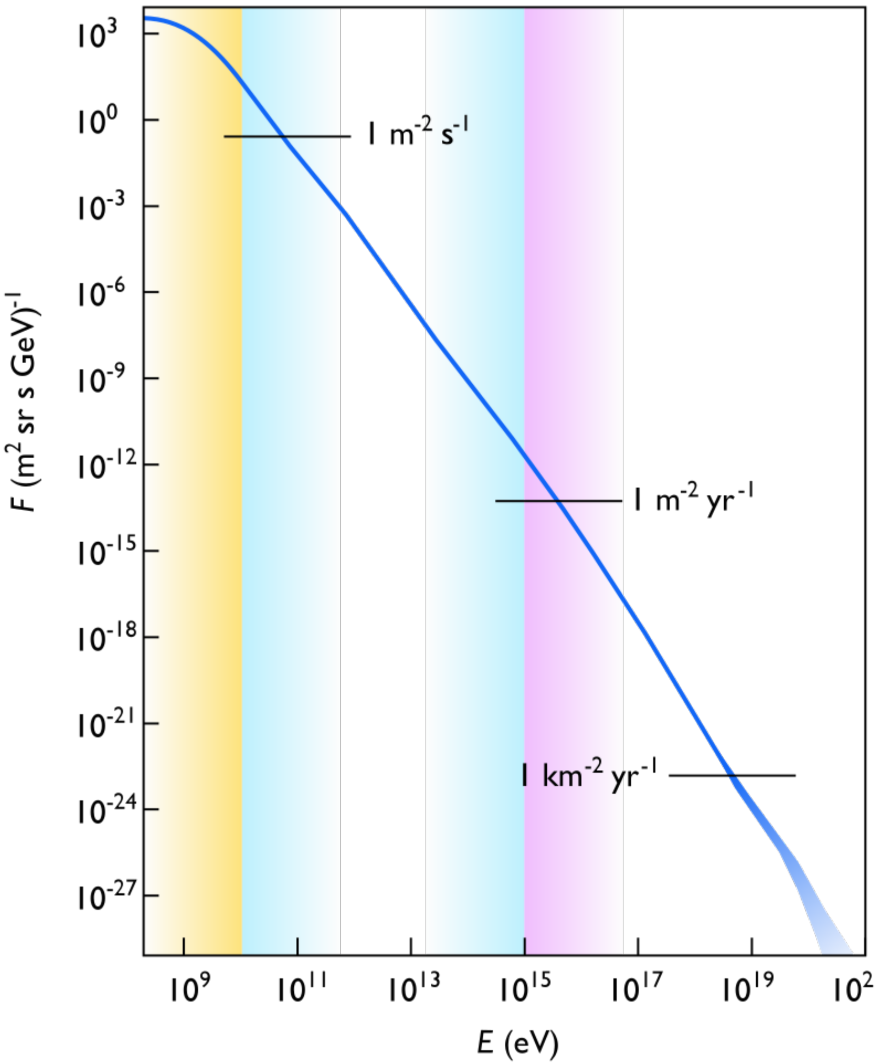

Fig: Cosmic flux versus particle energy at the top of Earth's atmosphere (credit: wikipedia)

What are the sources of the highest energy particles in our universe, the high-energy ($\geq 10^{15}$eV) cosmic rays ?

Neutrinos and gamma rays, a partnership to explore the extreme universe

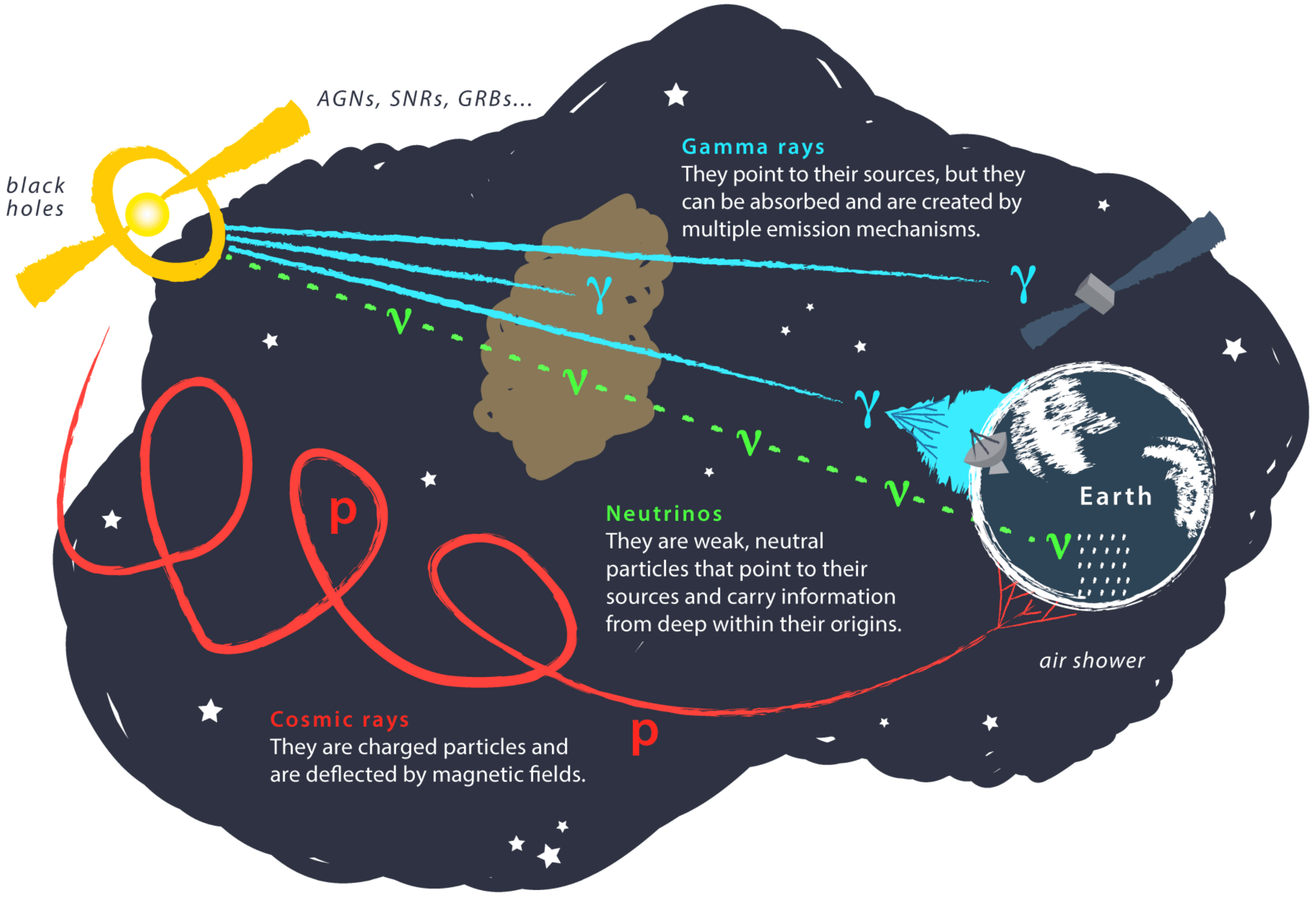

Image courtesy: Juan Antonio Aguilar and Jamie Yang. IceCube/WIPAC

How IceCube detects Neutrino?

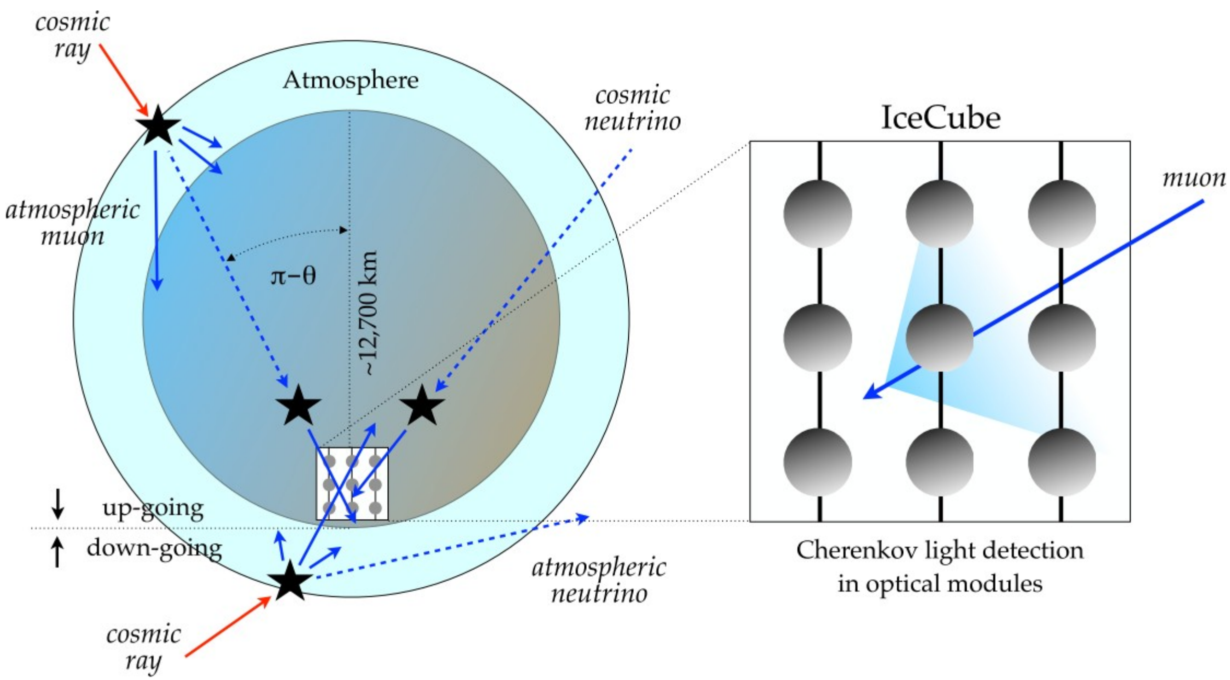

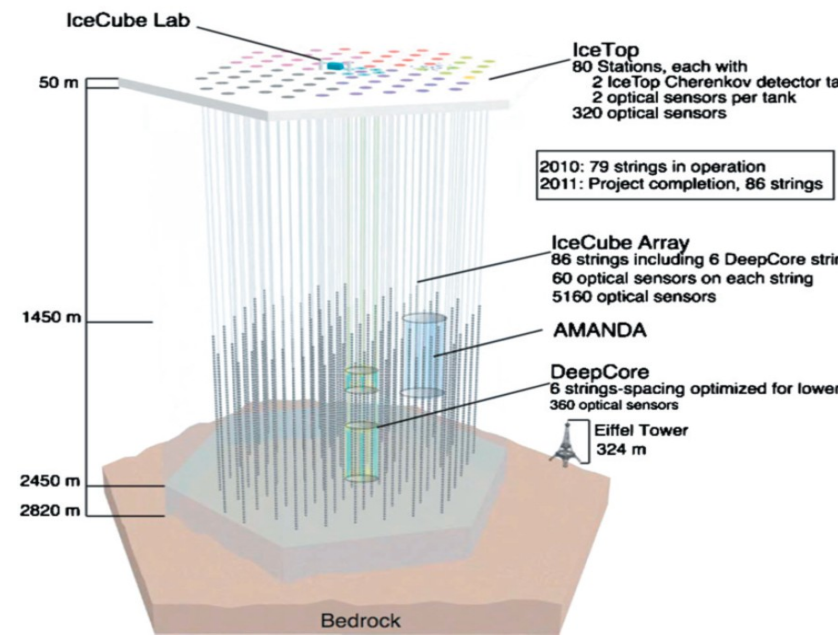

$$\nu_l + N \rightarrow l + \text{hadrons}$$ (Charged Current interaction)

$$\nu_l + N \rightarrow \nu_l + \text{hadrons}$$ (Neutral Current interaction)

Similar types of interactions happen for anti-neutrinos.

Courtesy: IceCube and High-Energy Cosmic Neutrinos Francis, Halzen & Kheirandish

Current status of the high-energy astrophysical neutrino sources

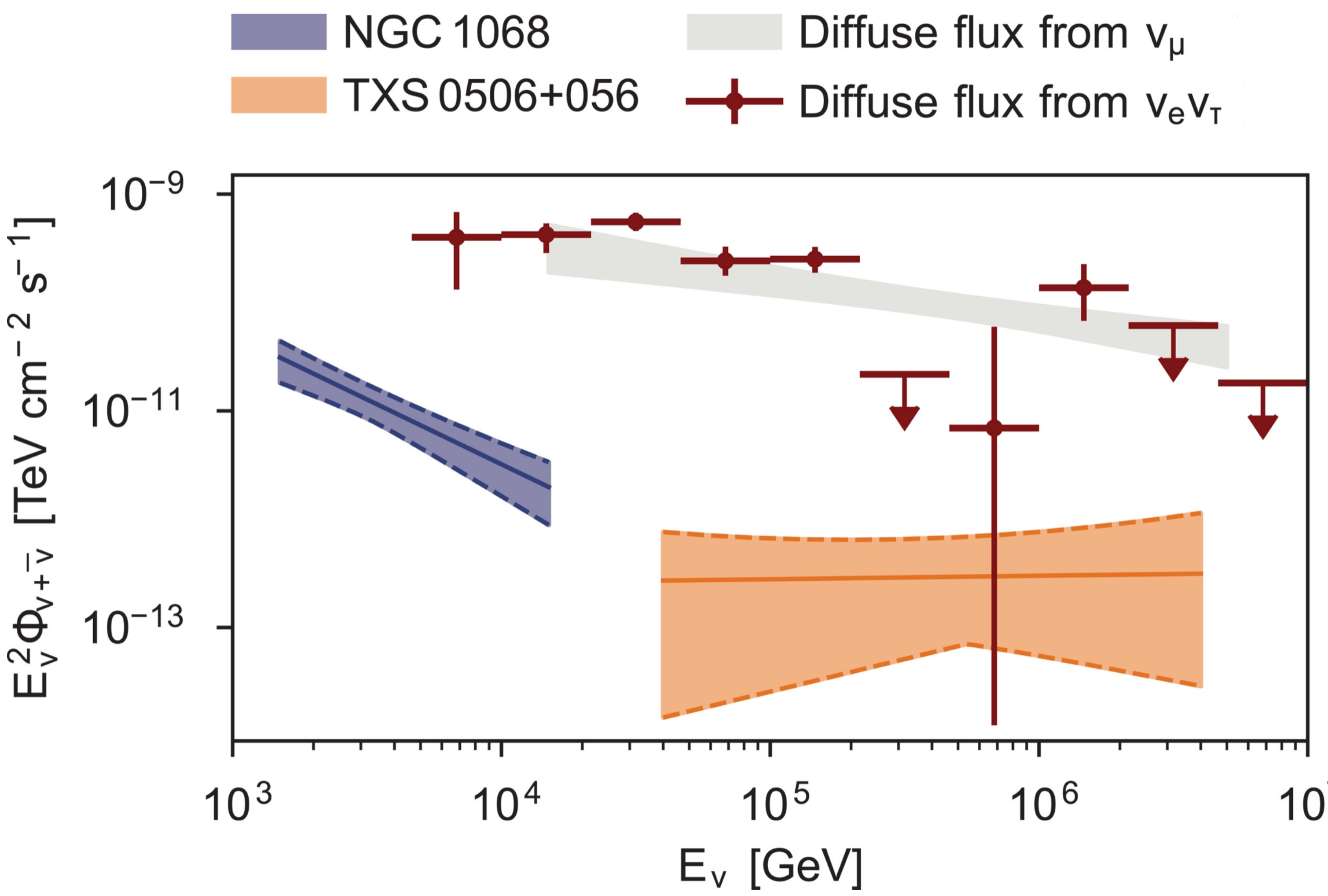

Fig: The high energy neutrino flux observed by IceCube. TXS 0506+056 and NGC 1068 are confirmed high-energy astrophysical neutrino sources till now. We also observe a high-energy diffuse astrophysical neutrino (in all flavors) flux. Currently, we do not know what sources contribute entirely to the high-energy diffuse astrophysical neutrino flux. [courtesy: 2211.09972]

Proposed Neutrino Sources

- Blazars [arXiv: 1904.06371, 2004.09686, 2007.12706, 2309.03115]
- Gamma-ray bursts [arXiv: 1101.1448, 1412.6510, 1601.06484, 1702.06868]
- Radio bright AGN [arXiv: 2103.12813]
- Pulsar wind nebulae [arxiv: 2003.12071]
- Choked Jet Supernovae [arXiv: 1706.02175, 1809.09610]
- Fast radio bursts [arXiv: 1712.06277, 2212.06702]

And many more classes of sources…

What are other powerful hadronic accelerators in the cosmos?

What are other powerful hadronic accelerators in the cosmos?

What if galaxy mergers are emitting high-energy neutrinos?

What are other powerful hadronic accelerators in the cosmos?

What if galaxy mergers are emitting high-energy neutrinos?

Theoretical papers:

1. Kazumi Kashiyama and Peter Meszaros [arXiv:1405.3262]
2. Chengchao Yuan et al. [arXiv: 1712.09754]
3. Chengchao Yuan et al. [arXiv: 1810.04155]

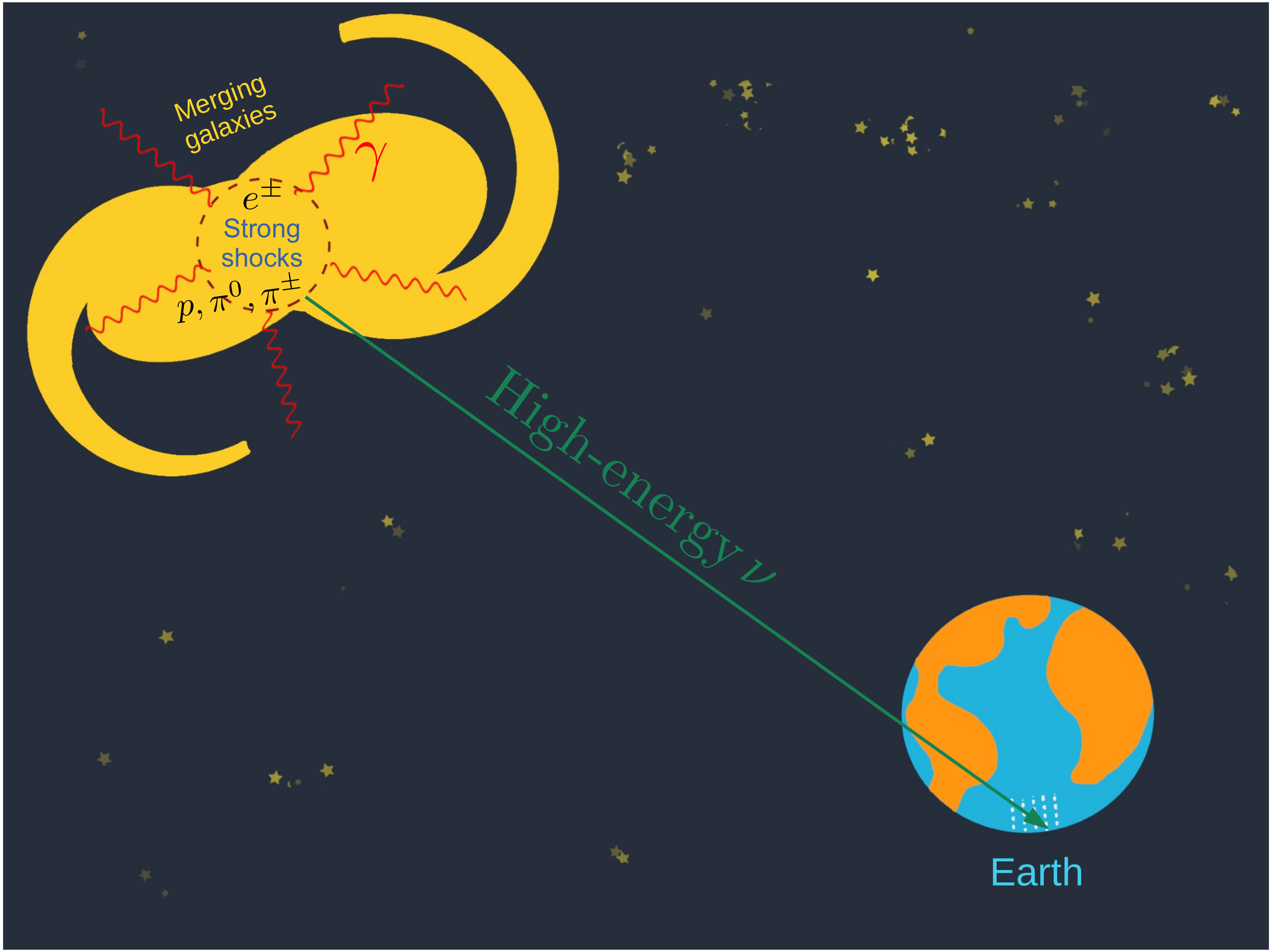

Fig: Schematic figure showing the merger of two galaxies. The shock is in the core region where interactions occur and neutrinos as well as electromagnetic radiation are produced.

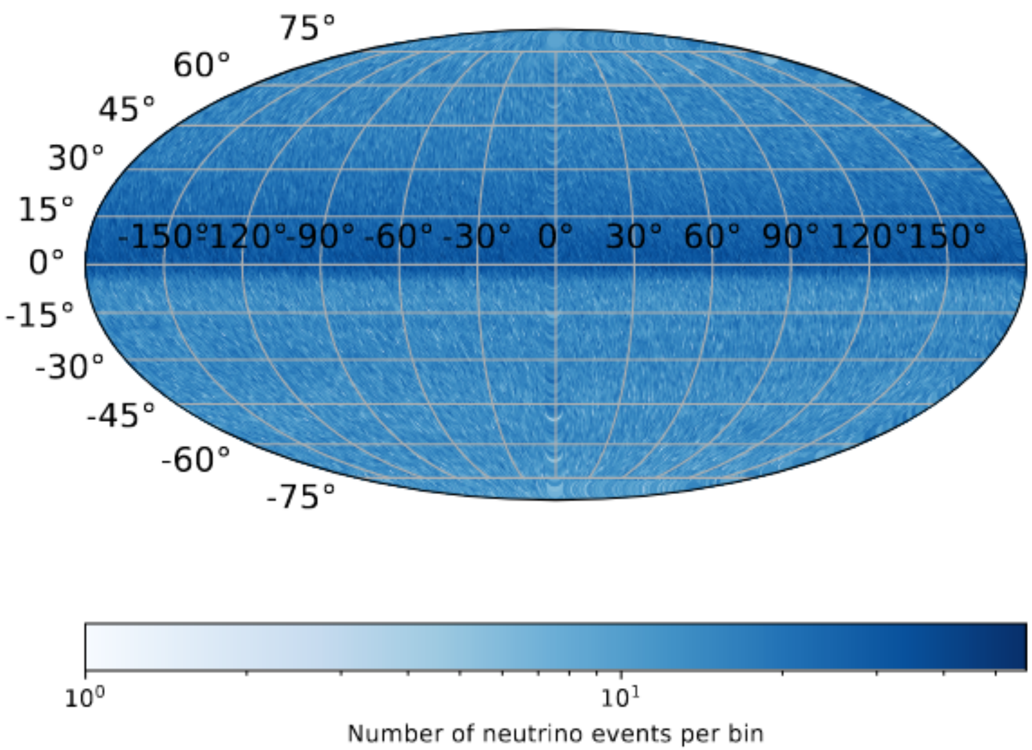

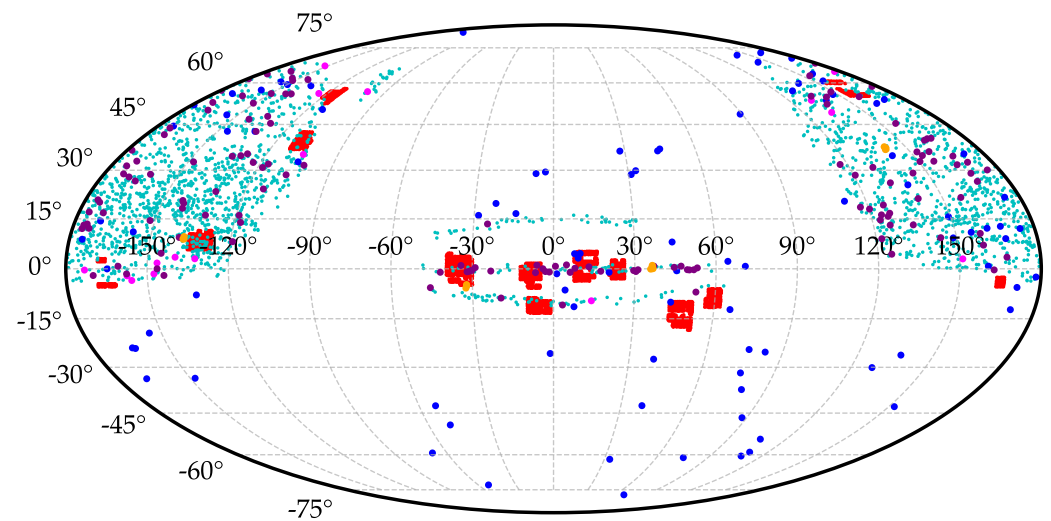

We look into the statistical correlation between the 10 years IceCube skymap and six galaxy mergers catalogs

Analysis Formalism

- Single Source Analysis

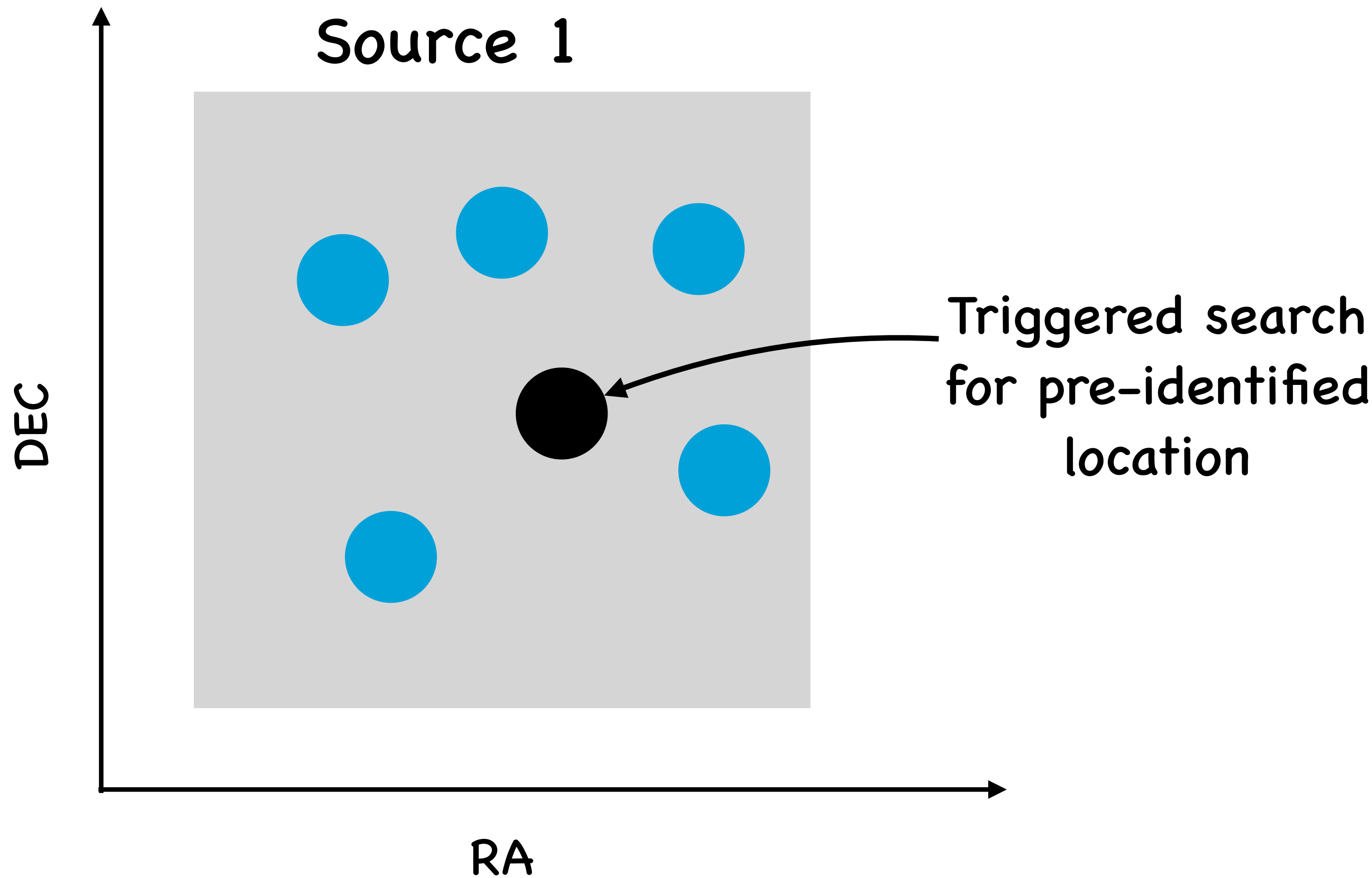

Fig: schematic representation of Single source analysis

Analysis Formalism

- Stacking Analysis

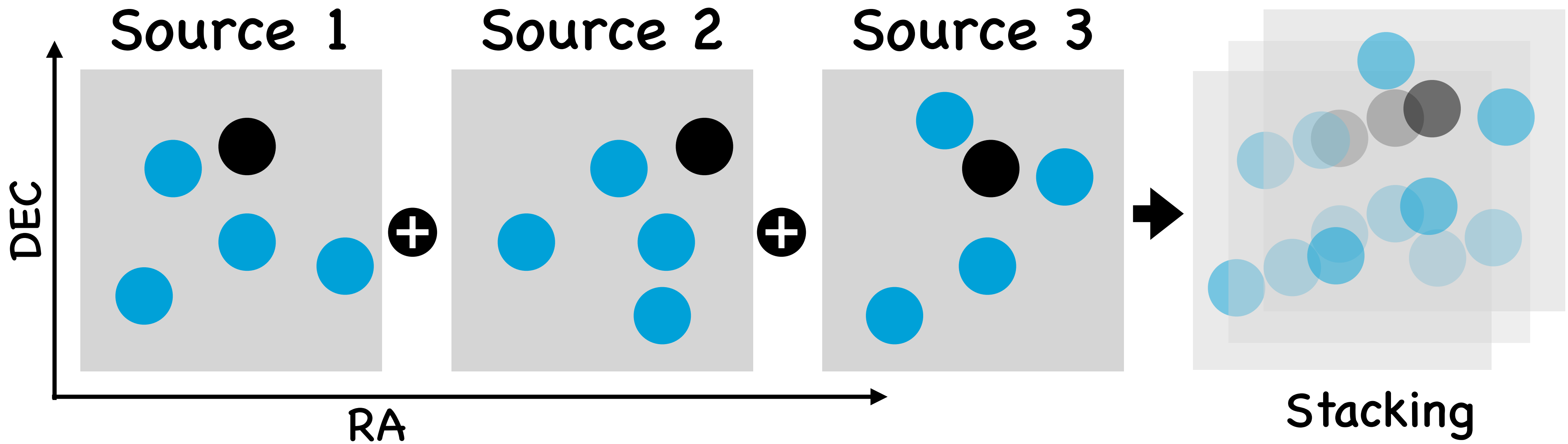

Fig: Schematic representation of Stacking analysis, search for collective neutrino emission from a catalog/class of sources

Analysis Formalism

- Test Statistic:

$$TS(n_s) = 2\,log\,\frac{\mathscr{L}(n_s)}{\mathscr{L}(n_S = 0)}$$

Hypothesis: neutrino events are coming from galaxy mergers

Null Hypothesis: all the events come from the background

- If the background hypothesis is true, the probability distribution for TS_{max} is approximately a χ^2 distribution.

$$\text{PDF}\,(TS_{max}) \approx \chi_1^2(TS_{max})$$

Results: Single Source analysis

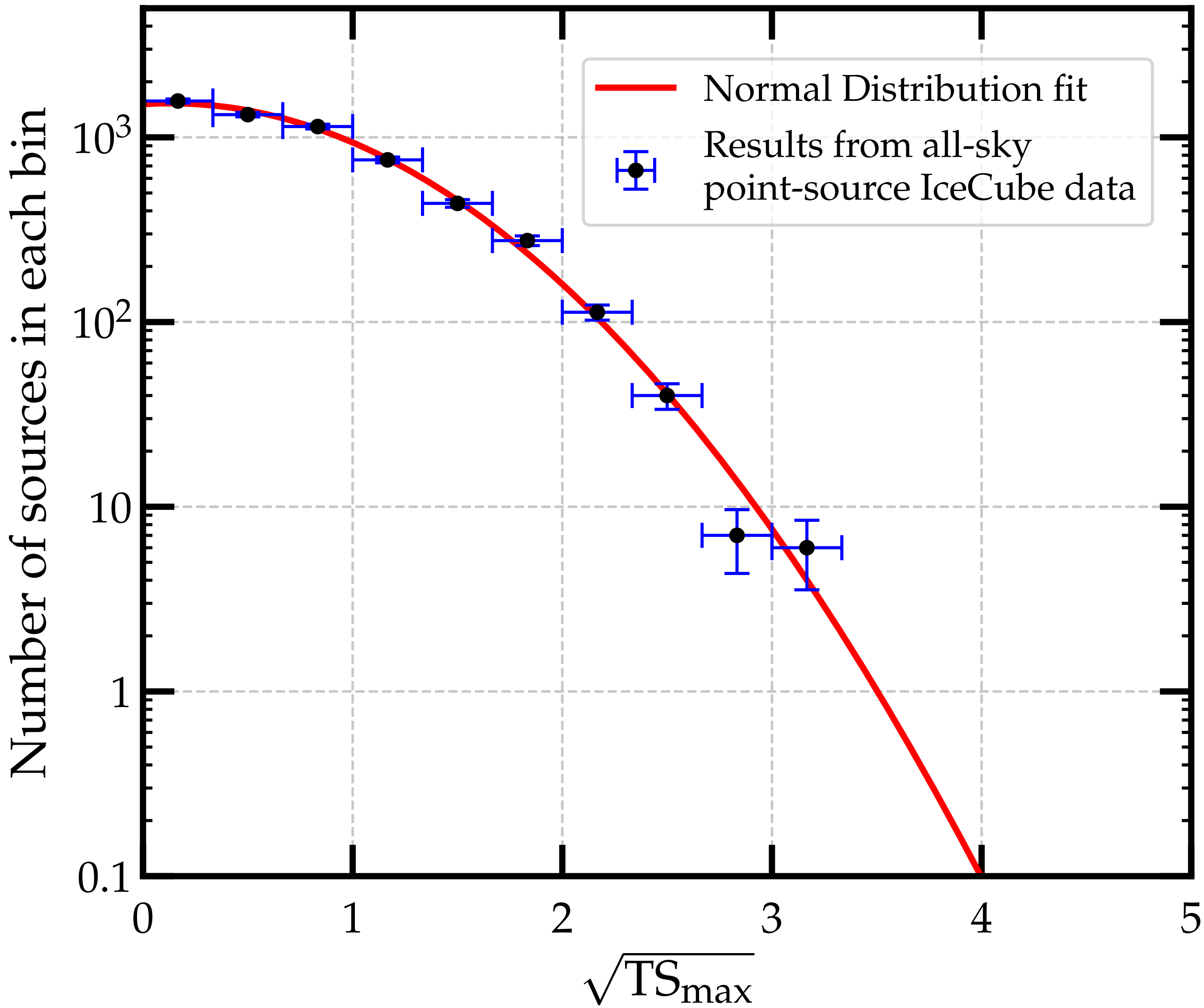

Fig: Distribution of square root of maximized TS values for all galaxy mergers from our likelihood analysis with 10 years of IceCube muon-track data. The normal distribution favours the null hypothesis implying high-energy astrophysical neutrinos are not coming from galaxy mergers. (Our work)

Results: Stacking Analysis

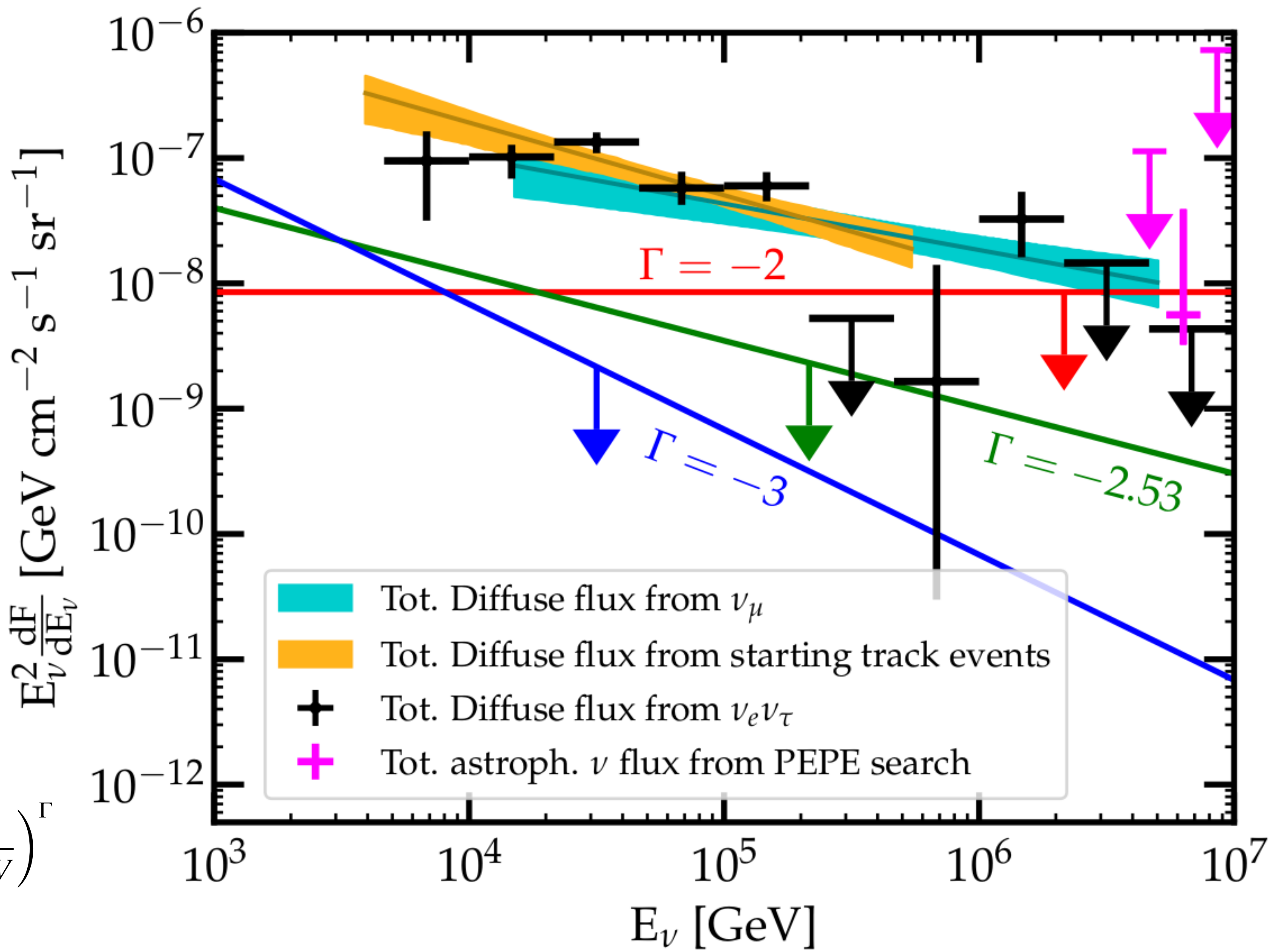

$$\phi = \phi_0 \left(\frac{E_\nu}{100\,TeV} \right)^{\Gamma}$$

Fig: All six-flavor neutrino energy fluxes vs. neutrino energy combining all the galaxy mergers in the six catalogs for the luminosity distance weighting scheme. The spectral index of signal neutrinos is Γ. (our work)

Conclusion

- We analyze the significance of each galaxy merger location in the six catalogs and find that none of the galaxy mergers in all six catalogs have a large global significance.
- Our stacking analyses show no significant correlation between our selected galaxy mergers and IceCube neutrinos with the current data set. For luminosity distance weighting, with $\Gamma = -2$, the upper limits can contribute no more than 19.69%, 17.08% and 16.88% of the total astrophysical diffuse flux observed by IceCube measured from muon-neutrino events, combined electron and tau neutrino cascade channels, and starting track events, respectively.

Conclusion

- We analyze the significance of each galaxy merger location in the six catalogs and find that none of the galaxy mergers in all six catalogs have a large global significance.
- Our stacking analyses show no significant correlation between our selected galaxy mergers and IceCube neutrinos with the current data set. For luminosity distance weighting, with $\Gamma = -2$, the upper limits can contribute no more than 19.69%, 17.08% and 16.88% of the total astrophysical diffuse flux observed by IceCube measured from muon-neutrino events, combined electron and tau neutrino cascade channels, and starting track events, respectively.

Thank you!

subhadipb@iisc.ac.in

Back Up Slides!

Results: Single Source analysis

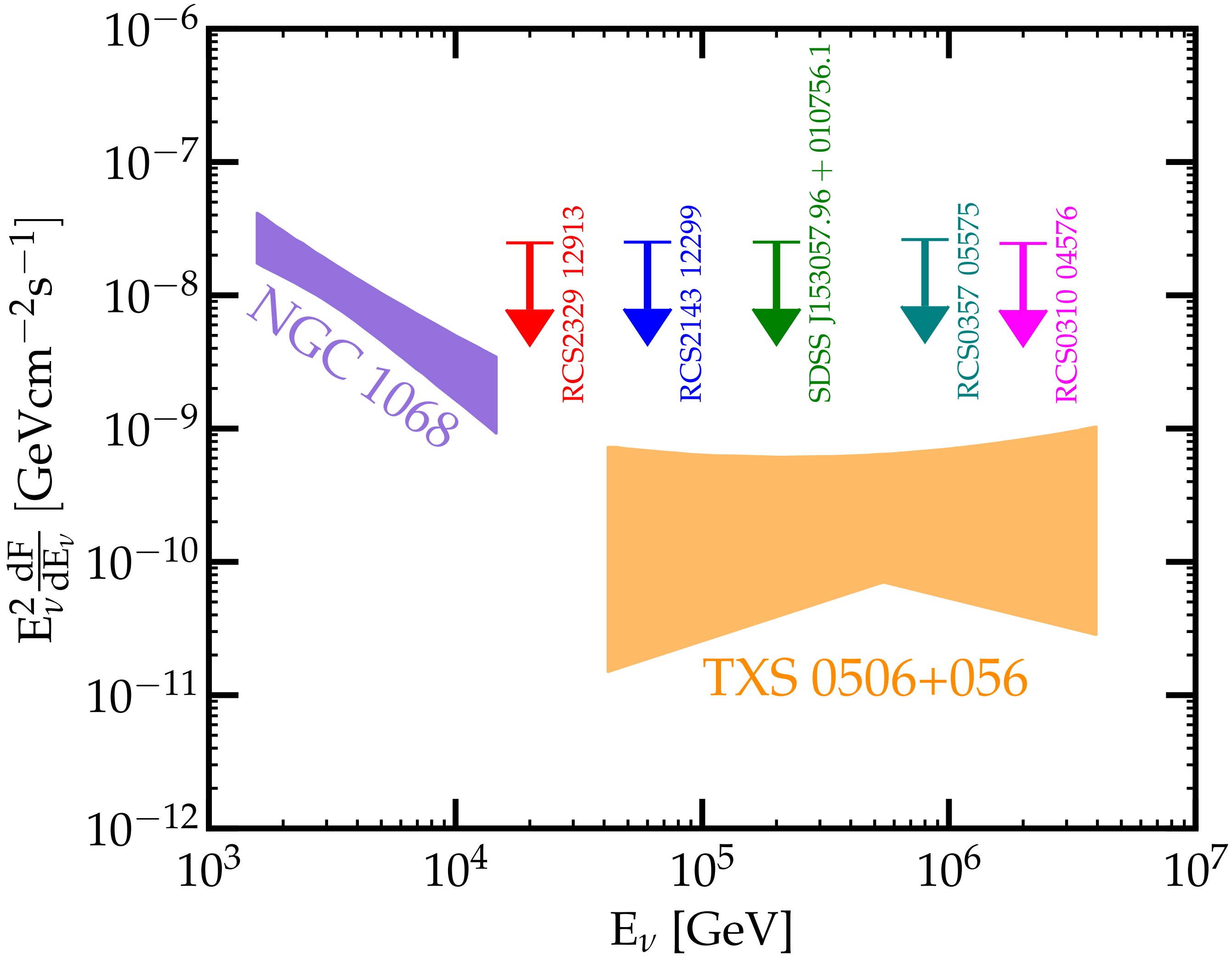

Fig: Upper limits on the total flux of high-energy neutrinos with $\Gamma=-2$ at various energies for the five most significant sources among all the considered galaxy mergers within six catalogs. (Our work)

Results: Single Source analysis

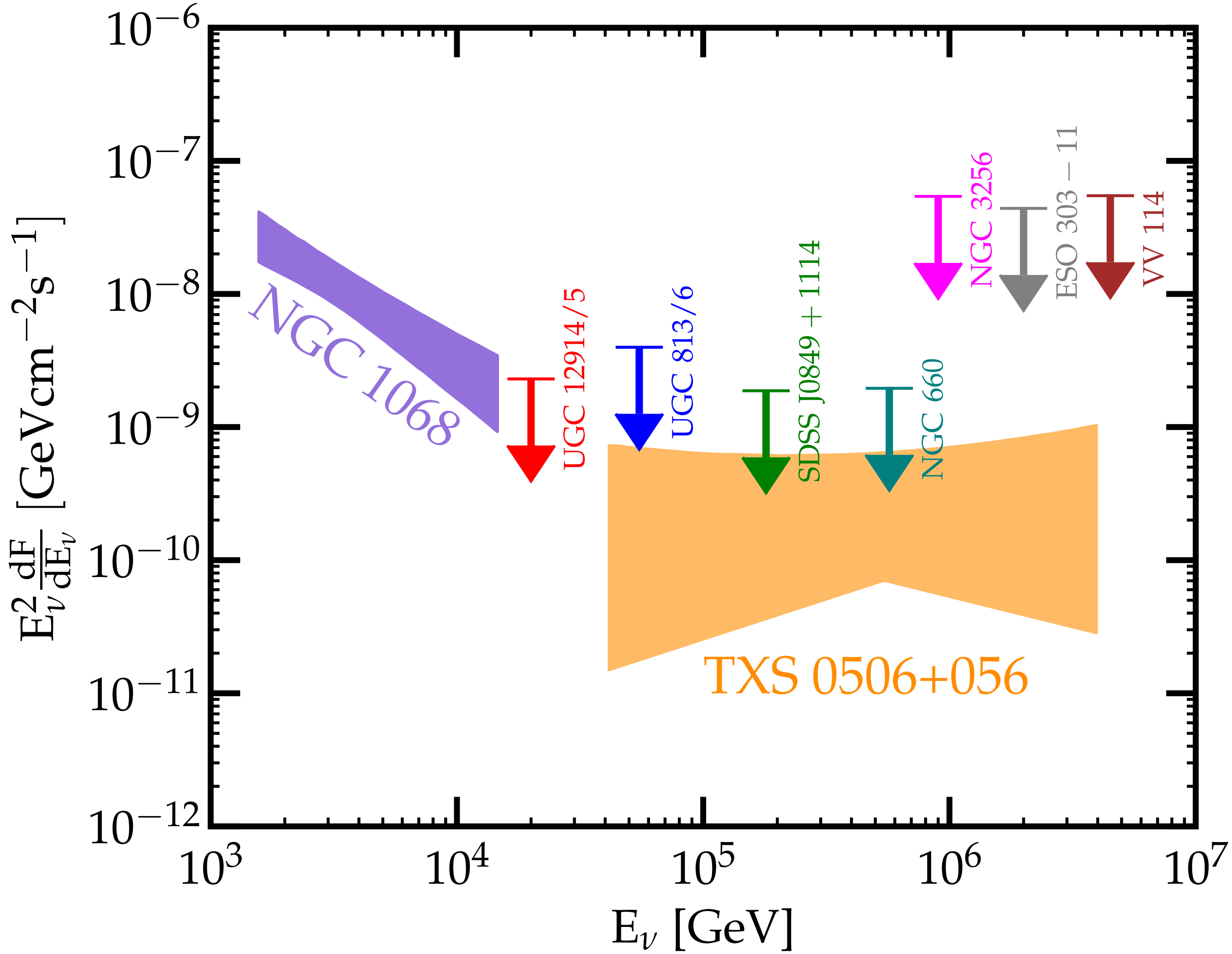

Fig: Upper limits on the total flux of high-energy neutrinos with $\Gamma=-2$ at various energies for seven interesting galaxy mergers mentioned in various references. (Our work)

Weighting Schemes for Stacking Analysis

- $w_{j,\text{model}} = 1$

- $w_{j,\text{model}} \propto 1/d_L(z)^2$

Luminosity Distance

- $w_{j,\text{model}} \propto \dfrac{\epsilon_\nu Q_\nu^{(g)}}{(1+z)^2 H(z)}$

All flavour luminosity density

Hubble parameter

[Taken from Yuan, Murase and Mészáros (arXiv: 1810.04155)]

Results: Stacking Analysis

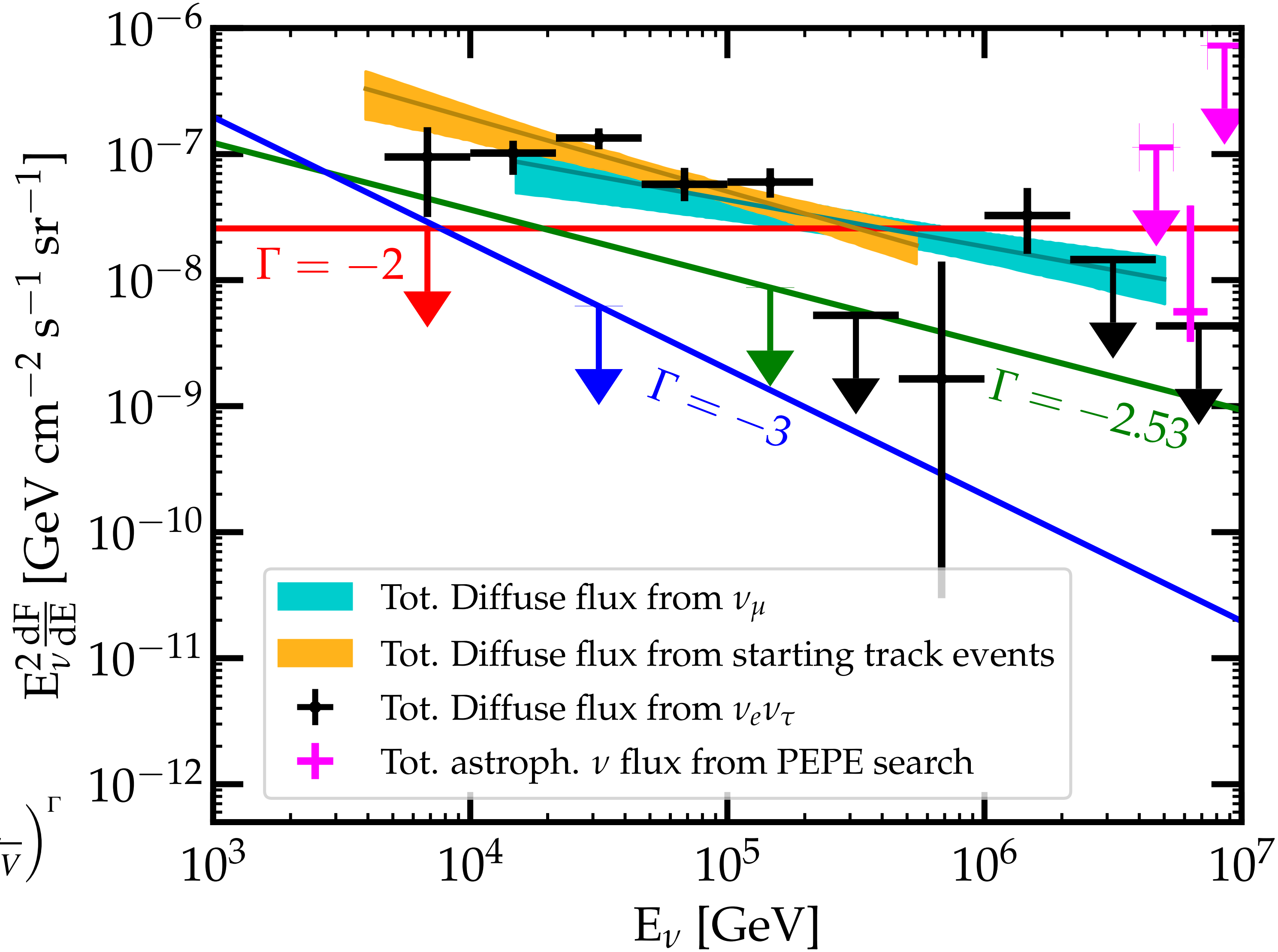

$$\phi = \phi_0 \left(\frac{E_\nu}{100\,TeV} \right)^\Gamma$$

Fig: All six-flavor neutrino energy fluxes vs. neutrino energy combining all the galaxy mergers in the six catalogs for equal weighting scheme. The spectral index of signal neutrinos is Γ. (our work)

Results: Stacking Analysis

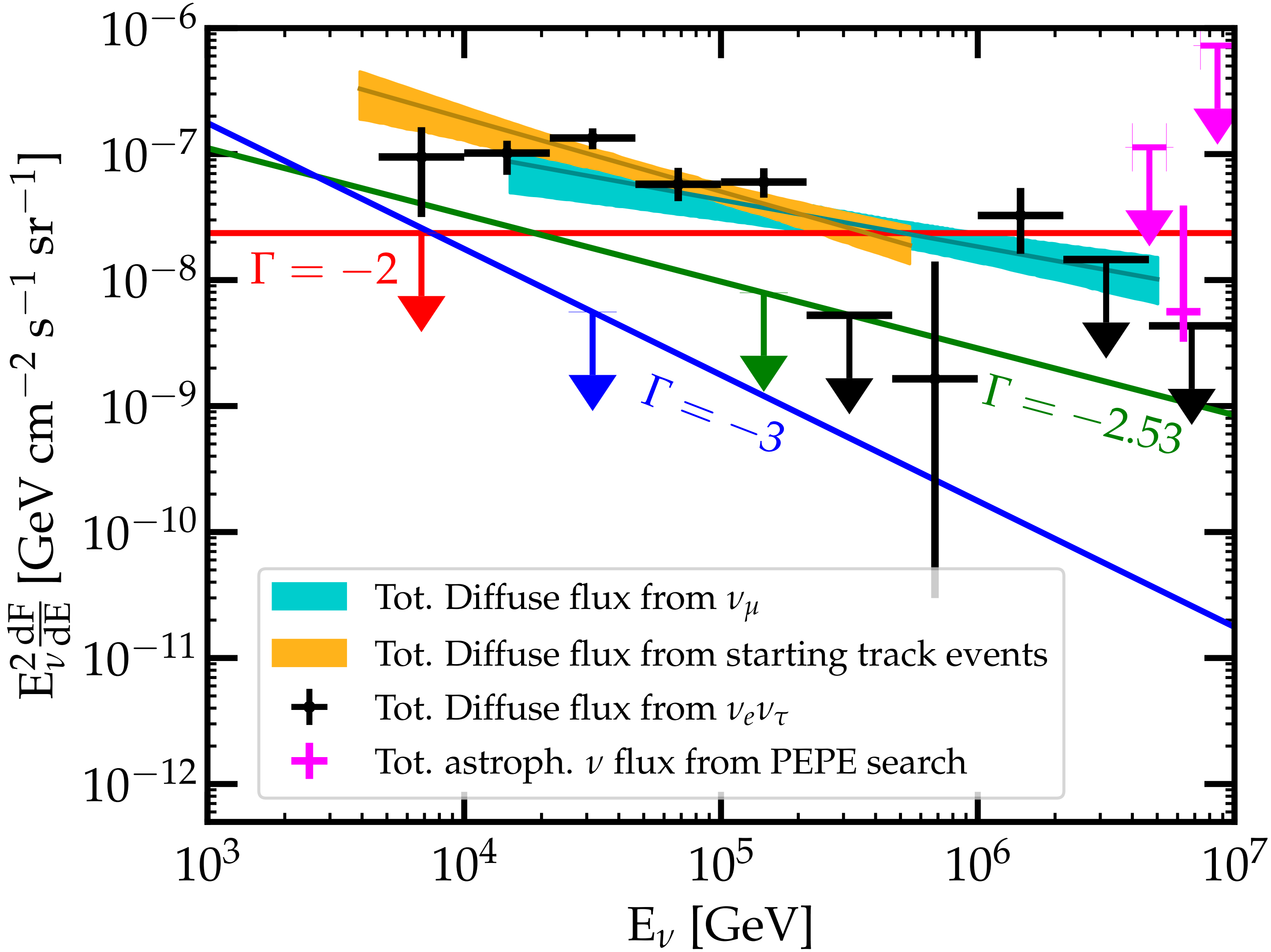

Fig: All six-flavor neutrino energy fluxes vs. neutrino energy combining all the galaxy mergers in the six catalogs for the Yuan et al. weighting scheme. The spectral index of signal neutrinos is Γ. (our work)

EBL

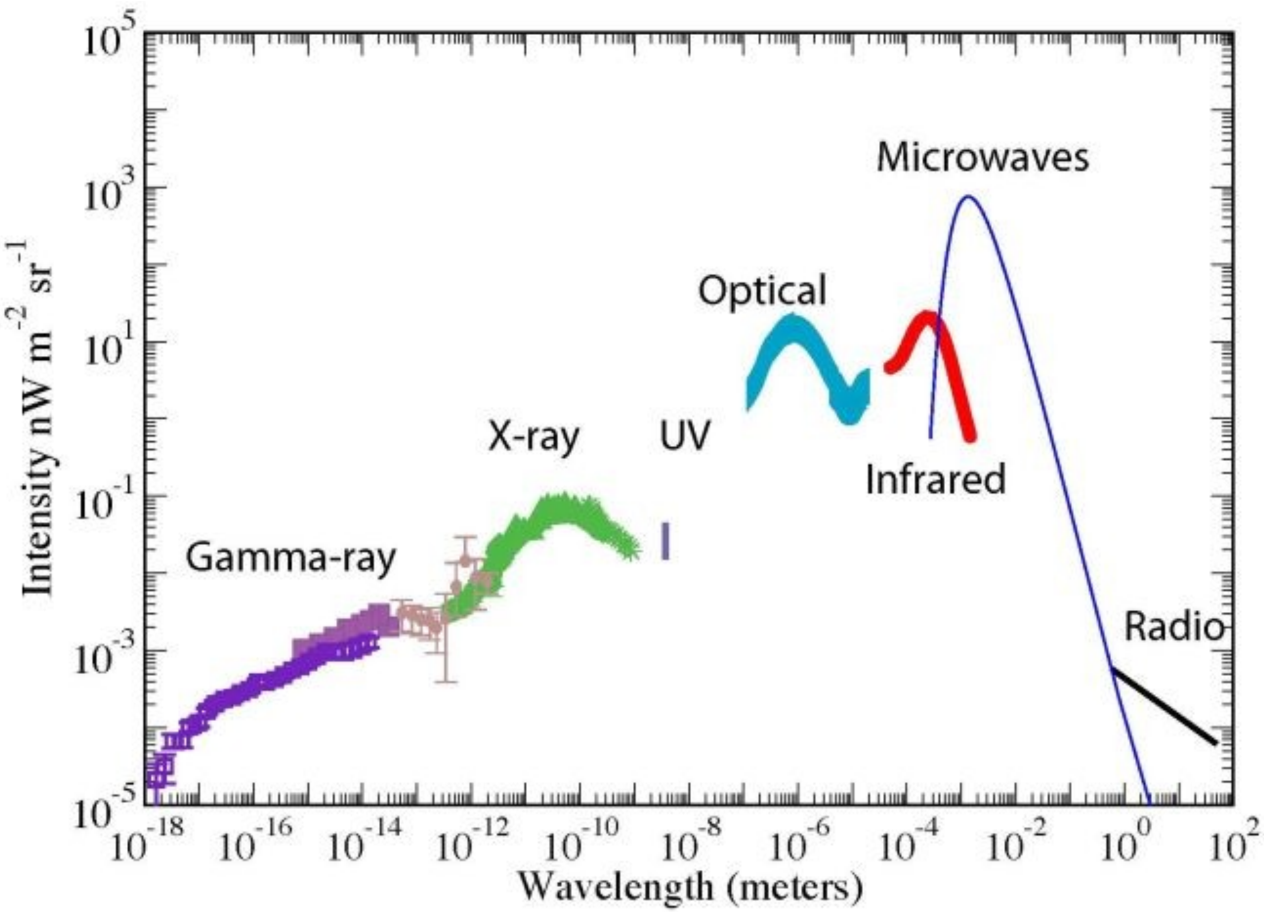

Courtesy: NASA

Pair production CC

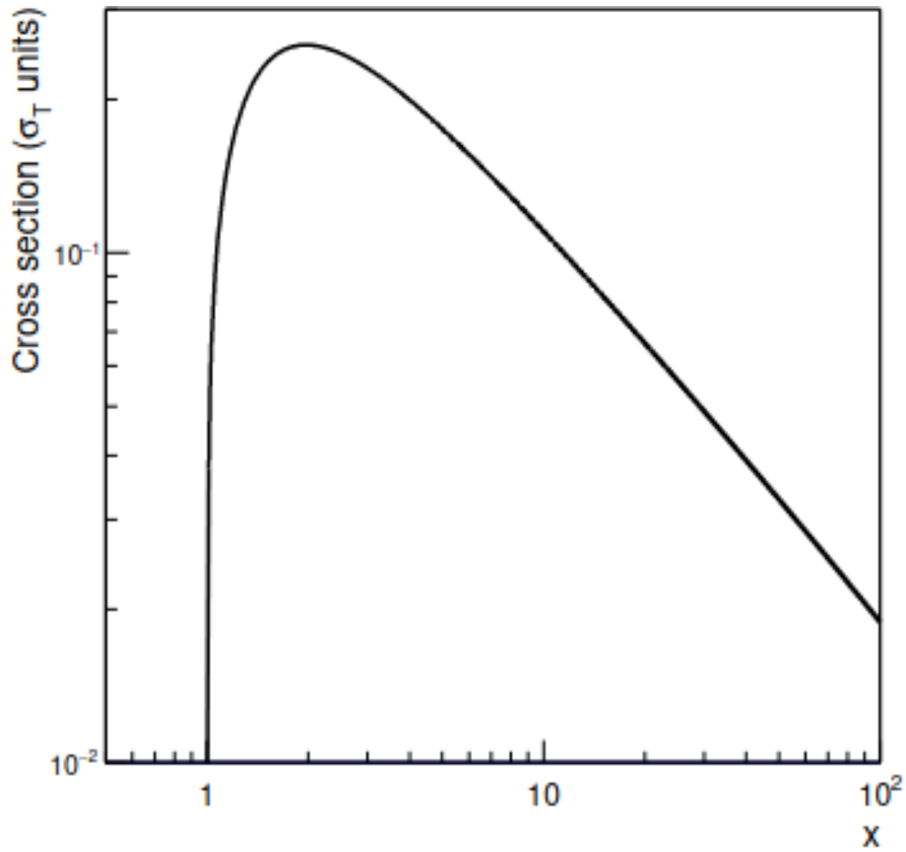

FIG. 1: Pair production cross section plotted as a function of the variable $x = s/(4m_e^2)$. σ_T is the Thomson cross section.

- $\sigma = (\frac{3}{16})\,\sigma_{Th}\,(1-\beta^2)\,[(3-\beta^4)\log(\frac{1+\beta}{1-\beta}) - 2\beta\,(2-\beta^2)]$, with $\sigma_{Th} = \frac{8\pi}{3}(\frac{\alpha}{m_e})^2 = 6.63081 \times 10^{-29} m^2$.
- β is the speed of the outgoing electrons in the center of mass frame of the process.
- β depends on the energy of the high energy photon, E, the background photon energy, ϵ, and the angle between their momenta θ and the mass of the electron.

More quantitatively,

$$\beta = \sqrt{1 - \frac{2m_e^2}{\epsilon E(1-\cos\theta)}} = \sqrt{1 - \frac{4m_e^2}{s}}$$

The cross-section has a threshold for the background field photon energy $\epsilon_{th} = \frac{2m_e^2}{E(1-\cos\theta)}$. Cross-section peaks at $\beta = 0.701317$ or $s = 1.9679\,(4m_e^2)$.

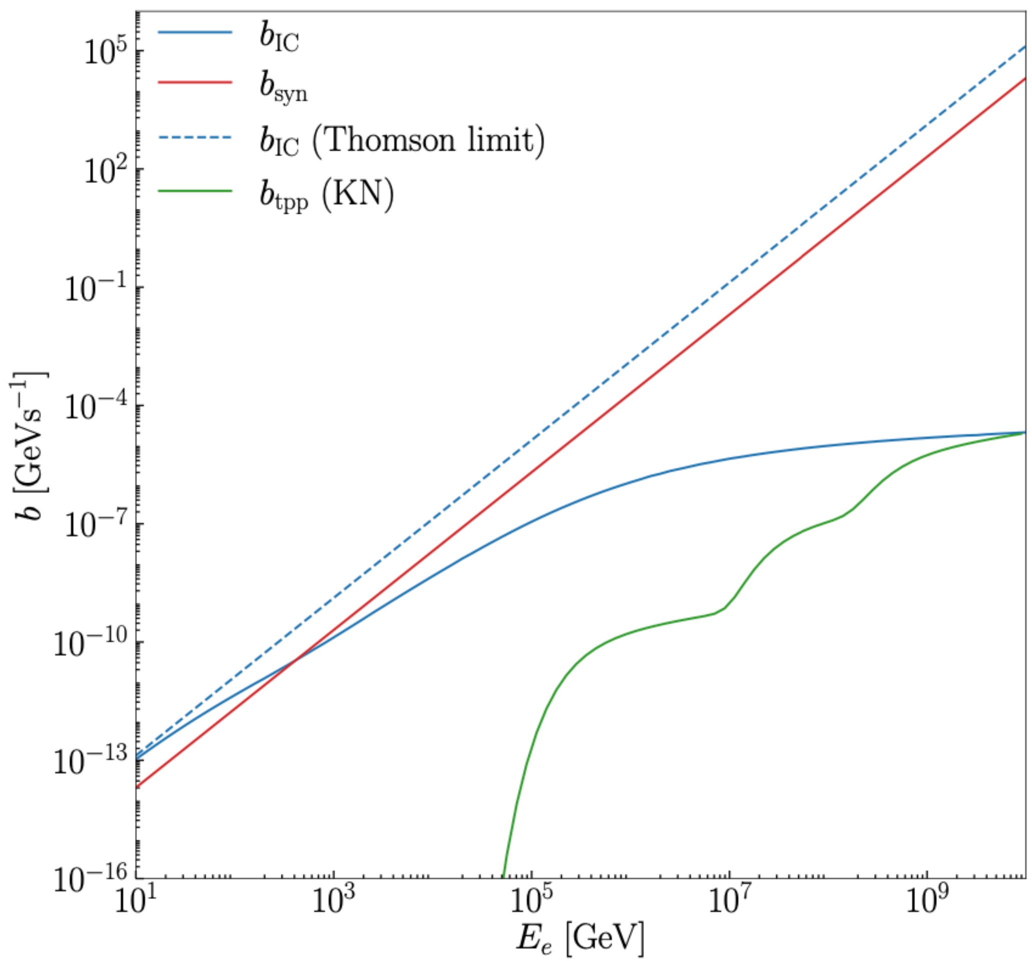

FIG. 1. Energy losses from synchrotron emission ($b_{\rm syn}$) from the Galactic Center, Inverse Compton emission ($b_{\rm IC}$), Inverse Compton emission in the Thomson limit ($b_{\rm IC}$ Thomson) and triplet pair production processses in the Klein-Nishina regime (b_{tpp} KN). At ultrarelativistic electron energies E_e close to half the DM mass $m_\chi/2$, synchrotron emission vastly dominates over IC and TPP emission.

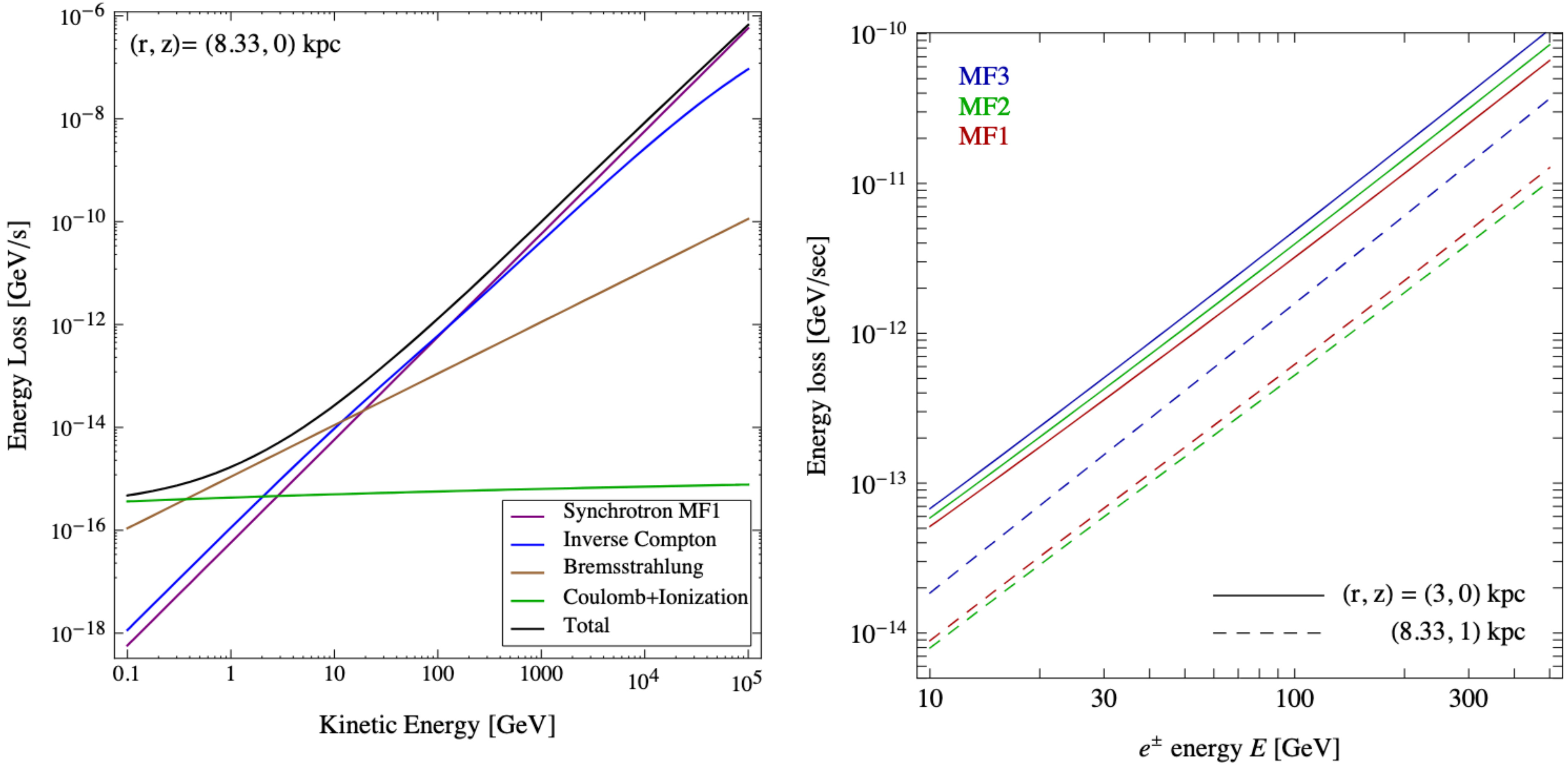

Figure 3: *Left panel: the* ***different processes*** *contributing to the energy loss function, at the location of the Earth. Right panel: the dependence of the energy loss coefficient function on the* ***choice of magnetic field model****, in two locations.*

Hillas Formula

$$E \approx Z e v B R$$

$$Z = 26 \qquad E = 10^{20}\,\mathrm{eV}$$

$$v = 0.99\,c$$

$$B = 10 \times 10^{-6} \times 10^{-4}\,\mathrm{T}$$

$$10^{22}\,\mathrm{eV} = 26 \times 1 \times 0.99 \times 10^{8} \times 3 \times 10^{-9} \times R$$

$$\Rightarrow R \approx 1.25 \times 10^{21}\ \mathrm{m}$$

$$\approx 41.96\ \mathrm{kpc}$$

$$\approx 8\ \mathrm{kpc}$$

$$\approx 16\ \mathrm{kpc}$$

$$\begin{aligned}
\varepsilon_\nu Q_{\varepsilon_\nu}^{(\mathrm{g})} =& \frac{1}{2}(1-e^{-f_{pp}^{\mathrm{g}}})\varepsilon_p Q_{\varepsilon_p}^{(\mathrm{LM})} \\
\varepsilon_\nu Q_{\varepsilon_\nu}^{(\mathrm{cl})} =& \frac{1}{2}[(1-e^{-f_{pp}^{\mathrm{cl}}})\varepsilon_p Q_{\varepsilon_p}^{(\mathrm{HM})} \\
&+ \eta(1-e^{-f_{pp}^{\mathrm{cl}}})e^{-f_{pp}^{\mathrm{g}}}\varepsilon_p Q_{\varepsilon_p}^{(\mathrm{LM})}],
\end{aligned}$$

$$\varepsilon_\nu^2 \Phi_{\varepsilon_\nu} = \frac{c}{4\pi}\int \frac{\varepsilon_\nu Q_{\varepsilon_\nu}^{(\mathrm{g})} + \varepsilon_\nu Q_{\varepsilon_\nu}^{(\mathrm{cl})}}{(1+z)}\left|\frac{dt}{dz}\right| dz\ , \qquad (18)$$

2018). Then, the effective *pp* optical depth is estimated to be $f_{pp}^{\mathrm{g}} = \kappa_{pp} c g(z) n_{\mathrm{g},0}\sigma_{pp}\mathrm{min}[t_{\mathrm{dyn}}, t_{\mathrm{diff}}] \simeq 0.24\ g(z)\left(\frac{n_{\mathrm{g},0}}{1\ \mathrm{cm}^{-3}}\right)\left(\frac{\sigma_{pp}}{50\ \mathrm{mb}}\right)\left(\frac{\mathrm{min}[t_{\mathrm{dyn}},t_{\mathrm{diff}}]}{10\ \mathrm{Myr}}\right)$ in the merging galaxy system. The ambient magnetic field en-

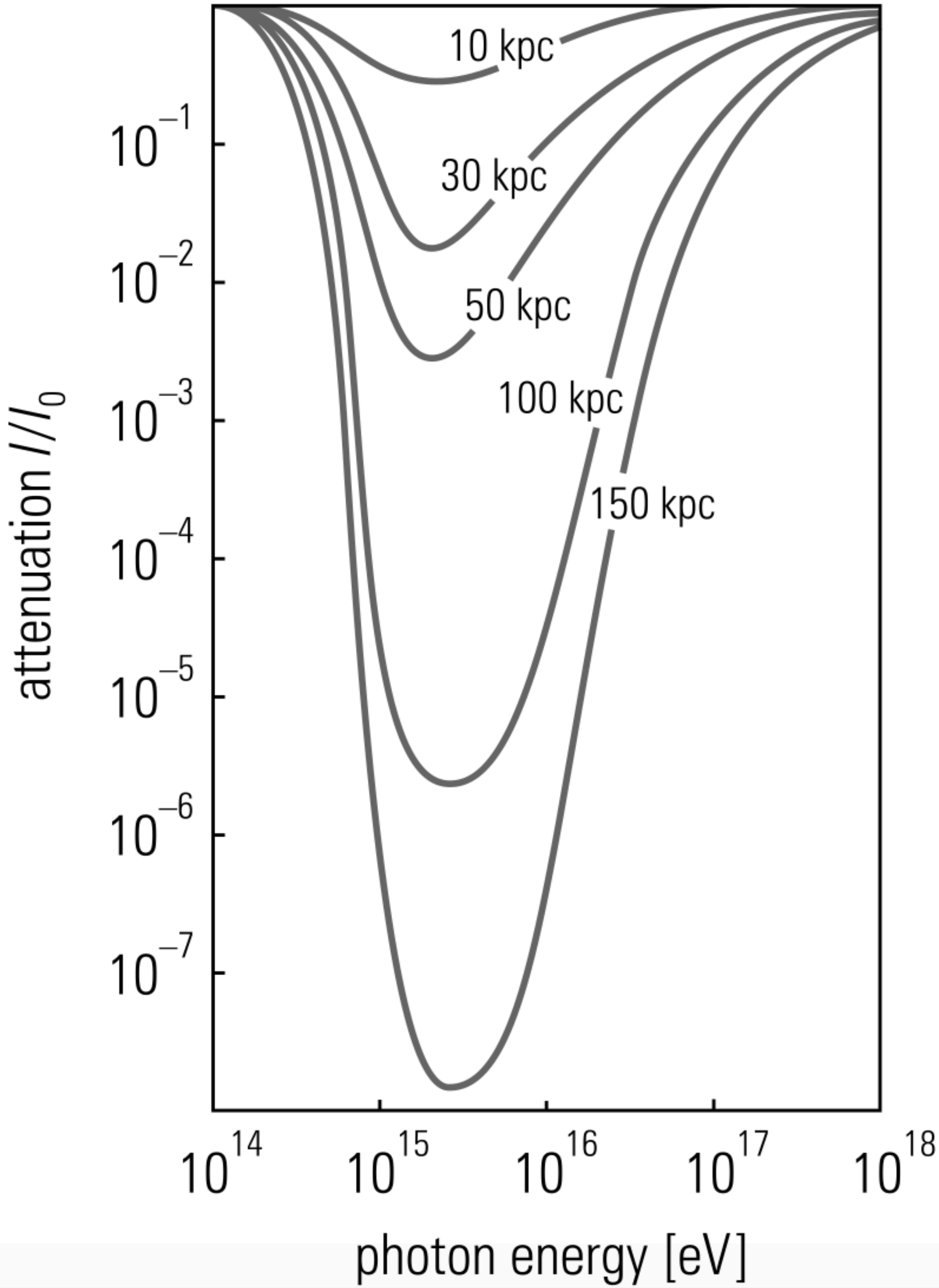
10 kpc
30 kpc
50 kpc
100 kpc
150 kpc
attenuation I/I0
10^{-1}
10^{-2}
10^{-3}
10^{-4}
10^{-5}
10^{-6}
10^{-7}
10^{14}
10^{15}
10^{16}
10^{17}
10^{18}
photon energy [eV]

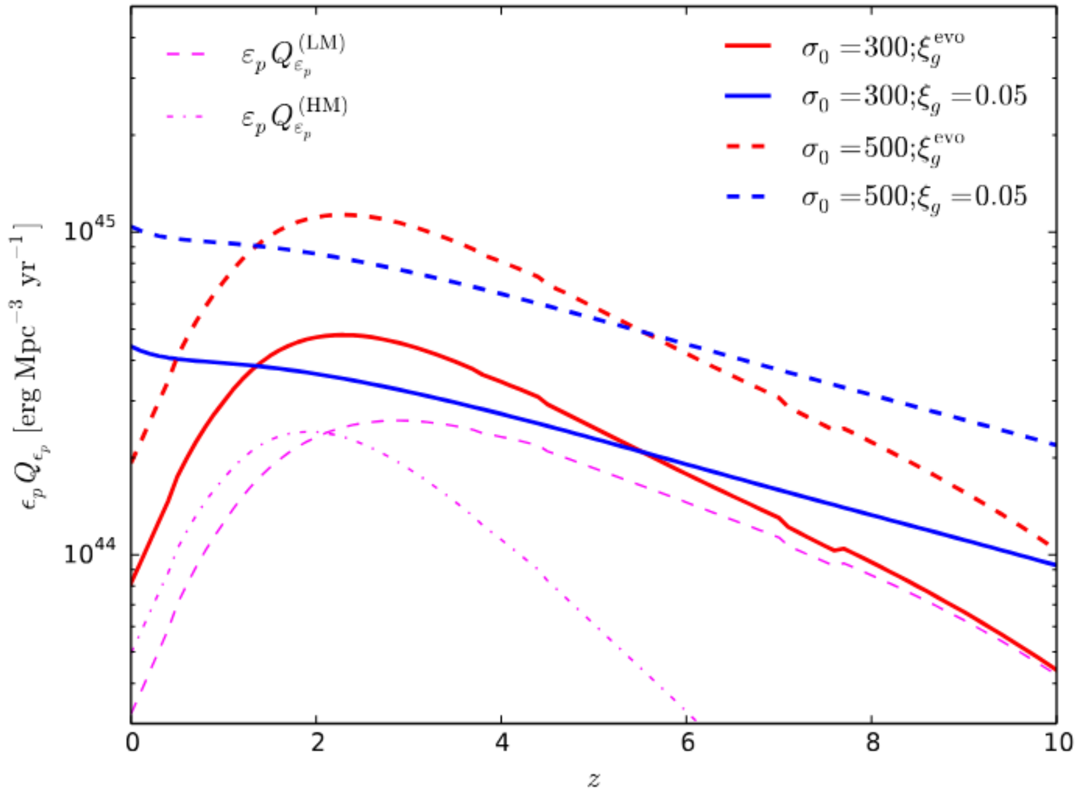

Figure 3. CR energy input rate versus redshift. The red lines correspond to a redshift-dependent gas fraction ξ_g^{evo} and the blue lines are for a redshift-independent gas fraction $\xi_g = 0.05$, while the solid lines are for $\sigma_0 = 300$ and the dashed are for $\sigma_0 = 500$, repectively. The dashed and dash-dotted magenta lines are LM and HM components of ($\sigma_0 = 300$, ξ_g^{evo}) scenario. Here LM and HM denote the low-mass (10^{10} $M_\odot - 10^{13} M_\odot$) and high-mass ($10^{13}$ $M_\odot - 10^{15} M_\odot$) intervals, respectively.

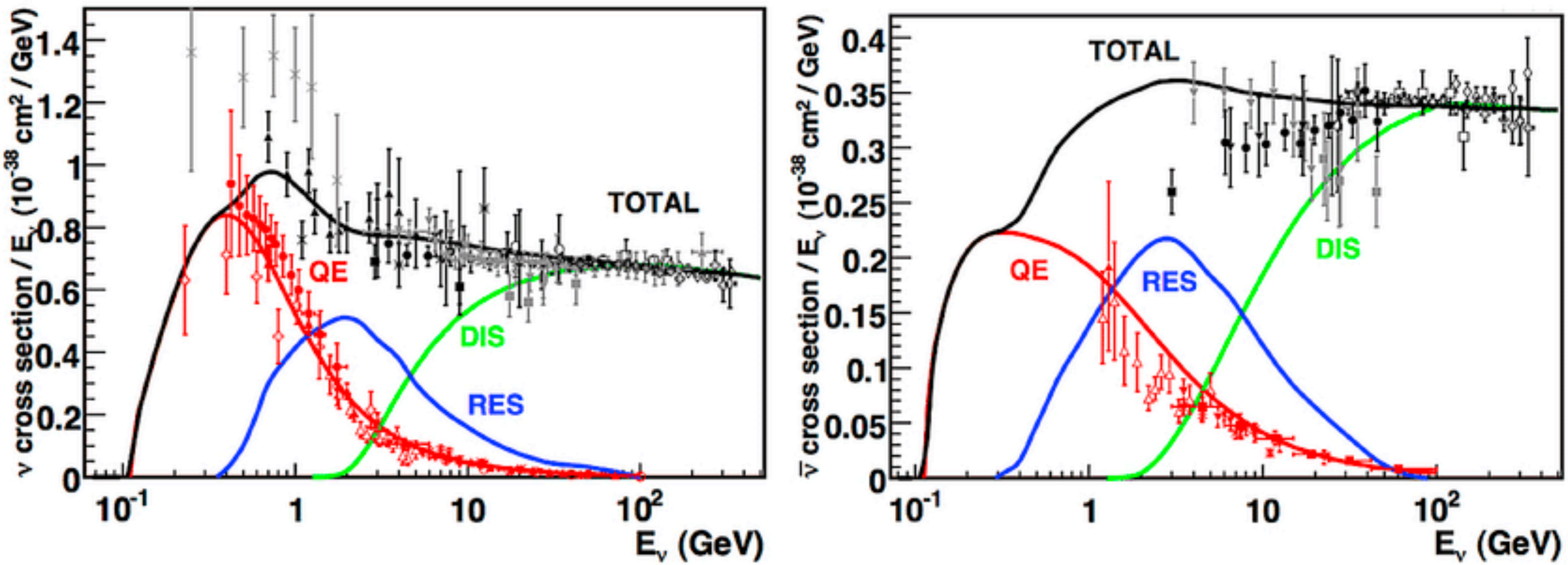
TOTAL
QE
DIS
RES
ν cross section / E_ν (10^{-38} cm^2 / GeV)
$\bar{\nu}$ cross section / E_ν (10^{-38} cm^2 / GeV)
E_ν (GeV)

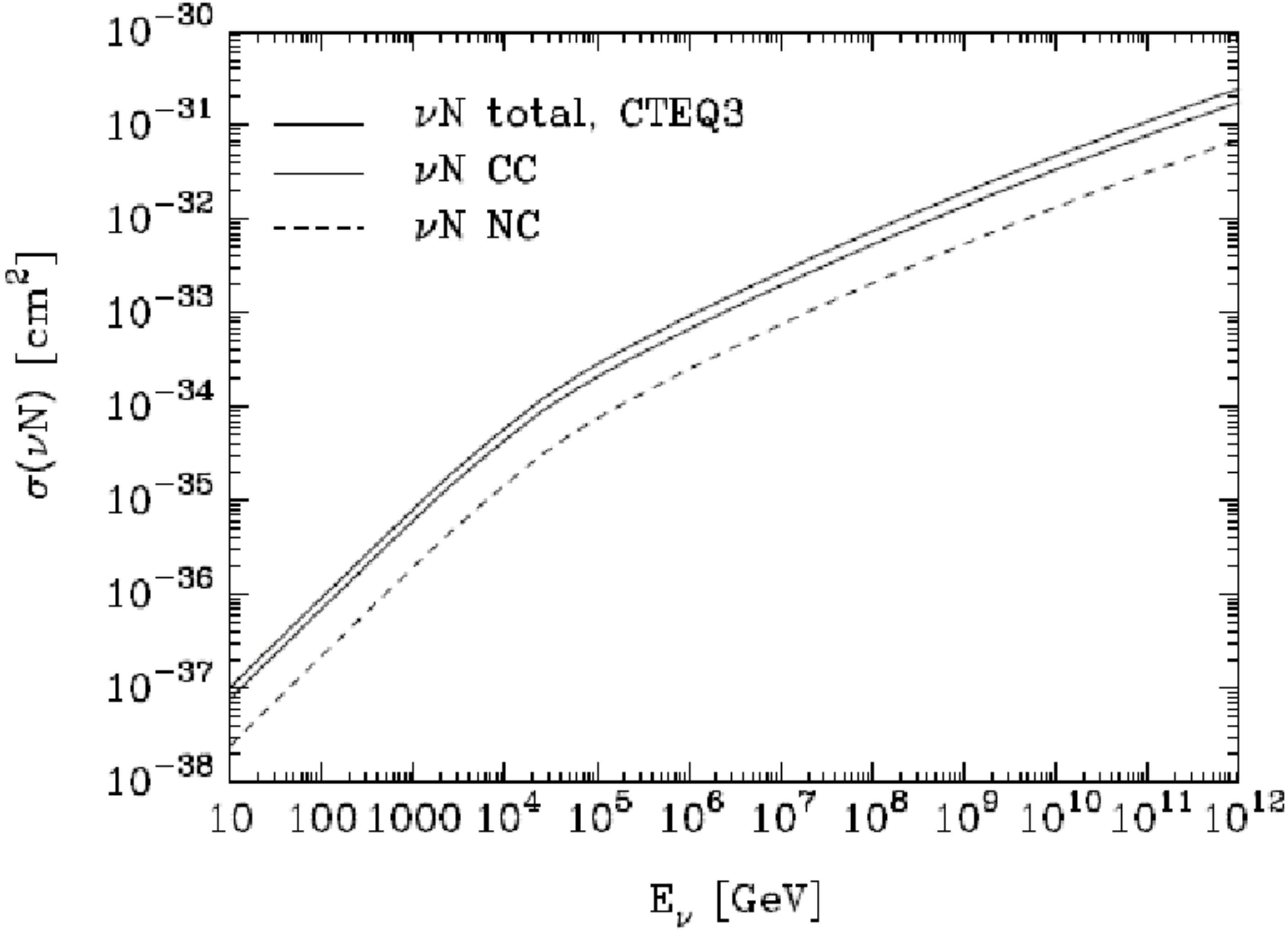

10^{-30}
10^{-31}
10^{-32}
10^{-33}
10^{-34}
10^{-35}
10^{-36}
10^{-37}
10^{-38}
$\sigma(\nu N)$ [cm^2]
νN total, CTEQ3
νN CC
νN NC
10
100
1000
10^4
10^5
10^6
10^7
10^8
10^9
10^{10}
10^{11}
10^{12}
E_ν [GeV]

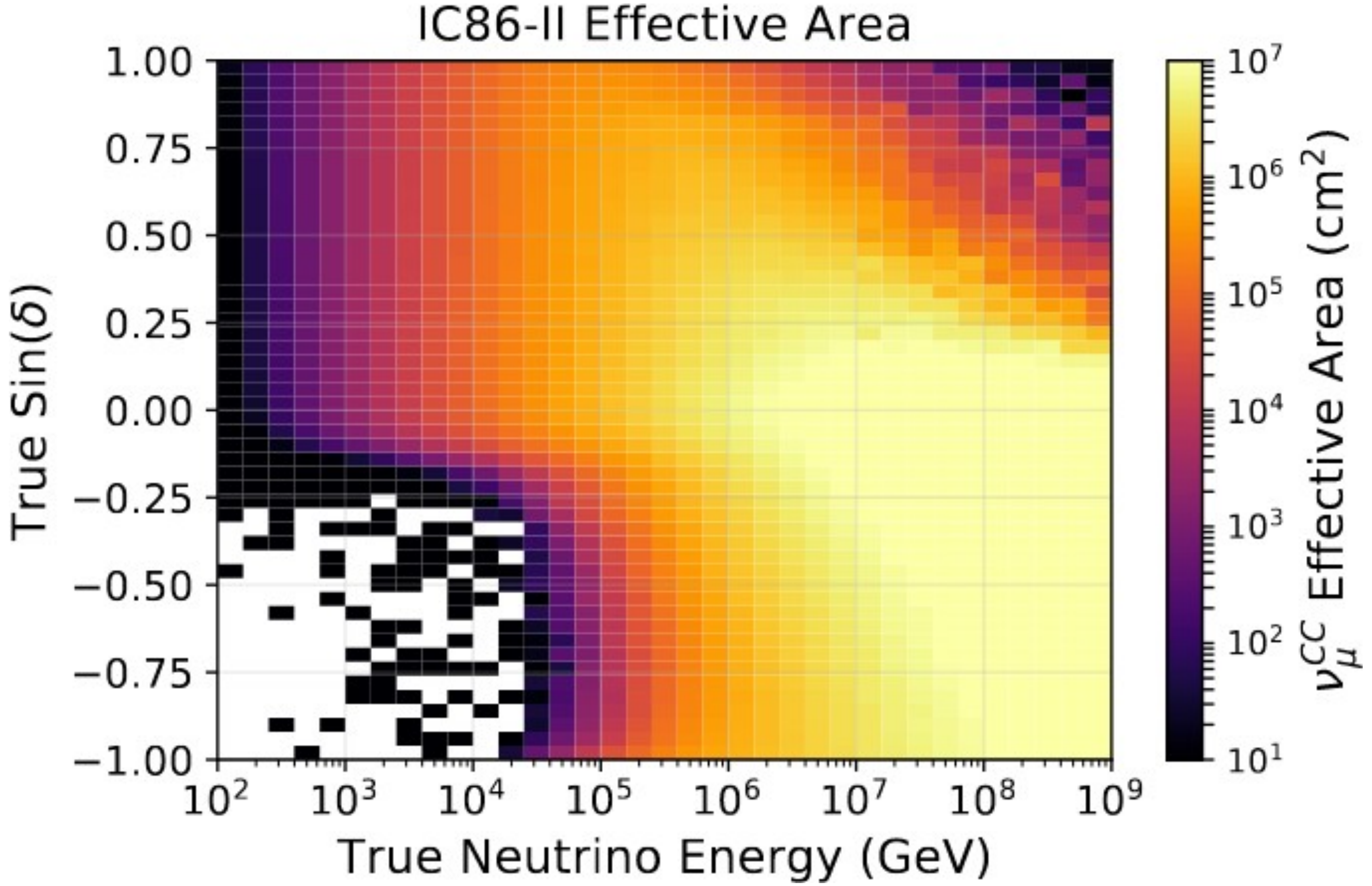

Courtesy: IceCube collab.

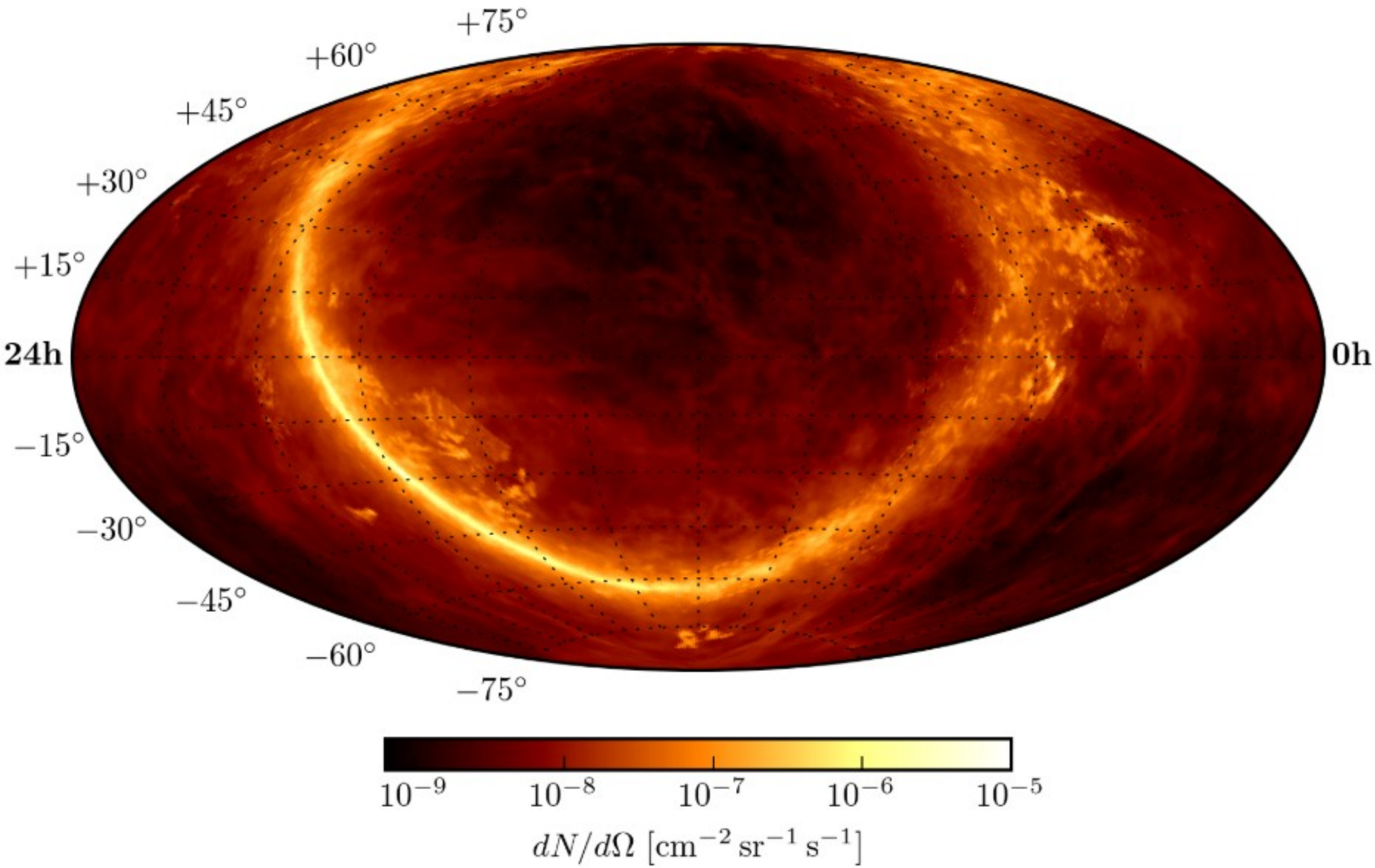

Diffuse galactic gamma ray flux